ELSEVIER

International Journal of Mass Spectrometry 223–224 (2003) 491–498

International Journal of Mass Spectrometry

www.elsevier.com/locate/ijms

An electrospray ionization—flow tube study of H/D exchange in protonated serine

Pavel Ustyuzhanin, Juliya Ustyuzhanin, Chava Lifshitz*

Department for Physical Chemistry and The Farkas Center for Light Induced Processes, The Hebrew University of Jerusalem, Givat Ram, 91904 Jerusalem, Israel

Received 27 November 2001; accepted 27 May 2002

Abstract

An electrospray ionization—fast flow technique has been employed to study the H/D exchange reactions of protonated serine with ND_3 and CH_3OD. A flow rate of 2.5×10^{17} molecules s^{-1} ND_3 at an overall pressure of 0.22 Torr and a reaction time of 21.4 ms is sufficient to exchange up to five labile hydrogens. With deuterated methanol raising the flow rate to 1.8×10^{18} molecules s^{-1} enabled observation of four exchanges and traces of a fifth exchange. Relative abundances for the various cations vs. neutral flow rates were measured. Optimum apparent and site-specific rate constants were deduced by simulated fits based on solutions of simultaneous first-order differential equations. Four site-specific rate constants deduced for the reaction of protonated serine with CH_3OD, 4.1×10^{-11}, 1.9×10^{-12}, 1.9×10^{-12}, and 1.9×10^{-12} cm^3 per molecule s^{-1} are very similar to the ones deduced for protonated glycine with CH_3OD. (Int J Mass Spectrom 223–224 (2003) 491–498)

Keywords: ESI; Flow tube; H/D exchange; Site-specific rate constants

1. Introduction

Lindinger's work has covered a very wide range of topics, from the very basic aspects of vibrational temperatures of diatomic ions [1] through ion/molecule reactions at near thermal energies [2] to on-line trace gas analysis at the pptv levels by means of proton transfer reaction mass spectrometry (PTR-MS) [3]. The majority of the work has been carried out using flow tube techniques with special emphasis on the SIFDT—selected ion flow drift tube in Innsbruck. PTR-MS has combined chemical ionization and in particular H_3O^+ formation and reactions with flow tube techniques.

There has been increasing interest in recent years in anhydrous protein and peptide ions [4]. We have combined electrospray ionization with a fast flow apparatus. This has opened the way for the study of ion/molecule reactions and H/D exchange of protonated biomolecules under thermal high-pressure conditions [5–10]. Our recent work on protonated L-serine to be described here is dedicated to Lindinger's memory.

Electrospray ionization mass spectrometry (ESI-MS) has been known [11] to produce multiply protonated peptides and proteins. The occurrence of 'fractional charging' by which cluster ions of amino acids are formed with more than one solute molecule per charge was discovered as well [12]. Large multimers were observed in the ESI-MS of peptides [13].

The formation of non-covalent supramolecular assemblies plays a critical role in biological systems. The discovery of multimers led to a series of studies of the clustering of the natural amino acids [14,15], the

* Corresponding author. E-mail: chavalu@vms.huji.ac.il

1387-3806/02/$ – see front matter
PII S1387-3806(02)00872-2

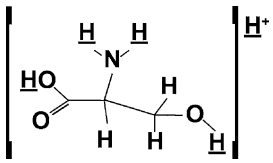

Scheme 1.

formation of peptide aggregates [16] and the complexation and clustering of proteins [17] under ESI-MS.

A fascinating discovery has been [15] that serine undergoes a chiroselective self-directed oligomerization to form a singly protonated octamer. Collision-induced dissociation that was performed led to the suggestion that the protonated octamer is composed of four hydrogen-bonded dimers, stabilized by further extensive hydrogen bonding. Density functional calculations supported this model.

Protonated serine is shown schematically in Scheme 1. The proton affinity and gas phase basicity of serine have been determined experimentally [18] to be PA = 218.6 kcal mol^{-1} and GB = 210.5 kcal mol^{-1}, respectively and by DFT calculations [19] PA = 218.3 kcal mol^{-1} and GB = 210.6 kcal mol^{-1}, in excellent agreement with experiment. The structures of six stable conformers were calculated for protonated serine [19]. The preferred site for protonation is the amino group. The lowest conformation shows an intramolecular hydrogen bond between NH_3^+ and the carbonylic oxygen. In addition, the oxygen atom of the side chain interacts as a proton acceptor with NH_3^+.

Protonated serine has five labile hydrogens that are underlined, Scheme 1. It is known to undergo H/D exchange with ND_3 when a BEqQ mass spectrometer is used [20]. These experiments were carried out at relatively high ion kinetic energies of a few electron volt. The present research concentrates on H/D exchange of thermal protonated L-serine ions.

2. Experimental

The electrospray ionization/fast flow apparatus is shown schematically in Fig. 1. It consists of a SIFT apparatus that we have constructed several years ago and modified to work with an electrospray (ES) source connected directly to the flow tube. The apparatus is made of a flow reactor that is 123 cm in length and an inner diameter of 74 mm. A neutral reagent is introduced into the flow tube through either one of two ring inlets. Tylan mass flow controllers define the flow rate of the neutral reactant into the flow tube. The quadrupole mass analyzer (652601 ABB EXTREL) is housed in a differentially pumped chamber that is separated from the flow tube by a nose cone (NC)

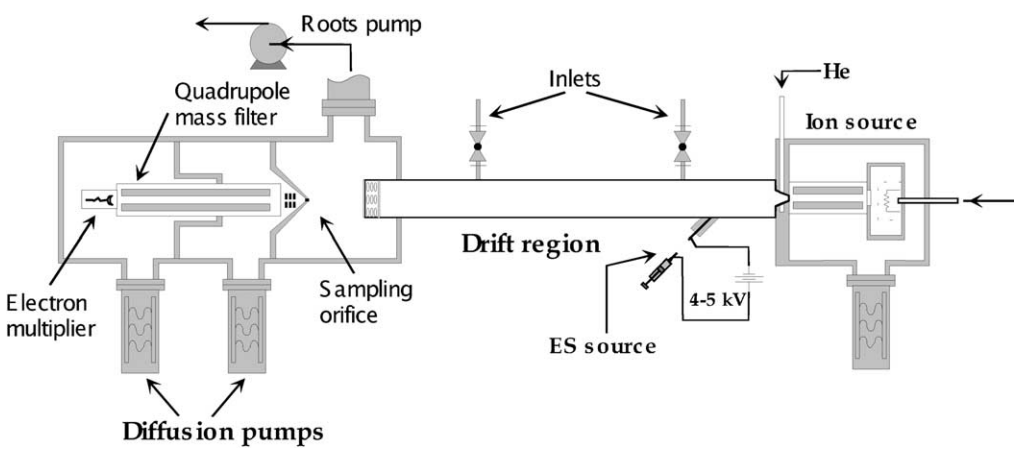

Fig. 1. Schematic drawing of the experimental setup combining electrospray (ES) ionization with a fast flow technique.

skimmer with a 1.0 mm sampling orifice. A small NC voltage is used for focusing ions into the analysis quadrupole. Helium buffer gas enters the flow tube at the upstream end near an electron impact ion source through another Tylan flow controller. It is pumped through the tube by a Roots blower with flow velocities of 2000–4500 cm s^{-1} leading to typical flow tube pressures ranging from 0.15 to 0.4 Torr and reaction times of several milli-seconds.

The electrospray ion source was designed as follows. A capillary tube serves as the interface between the electrospray and the helium flow reactor. Stainless steel tubes 15 cm in length and 0.05 cm i.d. are employed. The entire assembly is inserted into the flow tube at a distance of ∼96 cm from the sampling orifice, 135° to the direction of the helium flow, through an 'O'-ring type vacuum fitting. A capillary tube of 0.05 cm i.d. introduces an air leak into the flow tube with a pressure of 0.07 Torr and a flow rate of 1.3 L min^{-1} (STP); these numbers have to be added to the helium pressure and helium flow rate when calculating rate constants. Ions are electrosprayed ∼10 mm through ambient air into the grounded capillary tube from a stainless steel syringe needle biased at 5 kV DC. Dilute solutions of serine in a polar solvent are delivered to the electrospray needle at flow rates of 3–10 μL min^{-1} from a 5 mL syringe mounted on a model 100 KD Scientific Syringe Pump. The temperature of the capillary tube as well as of the flow tube does not exceed 26 °C.

The L-serine used in the experiments was purchased from Sigma/Aldrich (St. Louis, MO), with a stated minimum purity of 99%. ND_3 and CH_3OD were also from Sigma/Aldrich (St. Louis, MO), with a stated isotopic purity that exceeds 99% at. % D. Stock solutions of water–methanol (50:50), water–methanol–acetic acid (49:50:1), water–acetonitrile (50:50) and water–methanol–(0.01 M) NaOH (49:50:1) were prepared for this series of experiments.

The low resolution ESI mass spectrum of a water–methanol solution (0.1 mM) of L-serine at a nose cone voltage of 20 V is shown in Fig. 2. It demonstrates the monomeric ion $[M + H]^+$ at *m/z* 106 and a dimeric species $[2M+H]^+$ at *m/z* 211. About the same spectra

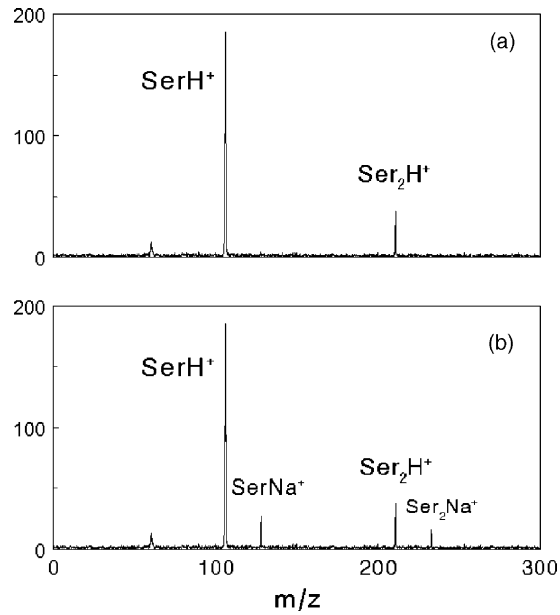

Fig. 2. Mass spectra obtained by the detector quad; (a) 0.1 mM of L-serine in a water–methanol (50:50) solution, (b) 0.1 mM of L-serine in a water–methanol–(0.01 M) NaOH (49:50:1) solution.

were obtained for most of the other solutions. The spectrum recorded under the same conditions for a solution that contains Na^+ ions demonstrates additional peaks of $[M + Na]^+$ at 128 *m/z* and $[2M + Na]^+$ at 233 *m/z*. It is well known that non-covalent complexes that are weakly bound are very sensitive to ion source conditions and to breakup due to collision-induced dissociations. Decreasing the nose cone voltage to 12 V leads to appearance of peaks corresponding to tetramers (*m/z* 421) and even to octamers (*m/z* 841). Unfortunately, adjusting our experimental conditions to see those multimers causes a general loss of intensity. This behavior is unlike that observed in experiments upon direct introduction of serine by ESI to a quadrupole ion trap mass spectrometer not via a flow tube [15]. We found that varying the concentration of serine in the range of 0.01–2 mM results in minor changes in the mass spectra. Under the experimental conditions specified the abundance of $[M + H]^+$ ions remained as the only measurable quantity of interest for which ion/molecule reactions could be run with confidence.

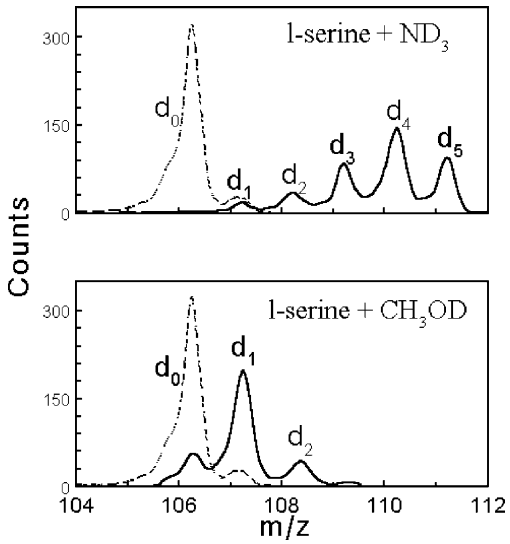

Fig. 3. Mass spectra (relative abundances vs. mass-to-charge (m/z) ratio) for protonated L-serine and its isotopic multiplet; in the absence of deuterating agent—dashed lines; with 2.5×10^{17} molecules s^{-1} ND_3—continuous line, top drawing; with 1.5×10^{17} molecules s^{-1} CH_3OD—continuous line, bottom drawing.

H/D exchange reactions were undertaken with ND_3 and CH_3OD. One set of results is represented in Fig. 3. A flow rate of 2.5×10^{17} molecules s^{-1} ND_3 at an overall pressure of 0.22 Torr and a reaction time of 21.4 ms (Fig. 3) is sufficient to exchange up to five labile hydrogens. With deuterated methanol raising the flow rate to 1.8×10^{18} molecules s^{-1} enabled observation of four exchanges and traces of a fifth exchange.

3. Data analysis

3.1. Deconvolution of mass spectral data

The elemental formula of protonated serine is $C_3H_8NO_3$. The isotopic multiplet of $(\text{serine} + H)^{1+}$ is observed to shift to higher masses (Fig. 3) upon introduction of ND_3 into the flow tube. The measured peaks are made up of contributions from undeuterated serine and its mono, di, tri, tetra and pentadeutero isotopomers. The undeuterated ion and its deuterated isotopomers each contribute a multiplet of isotopic peaks due to the natural abundances of the various carbon, nitrogen, oxygen and hydrogen isotopes. The isotopic natural abundance distribution complicates the analysis of the deuterium labeling data. Successful interpretation of the experiments requires removal of the isotopic natural abundance distribution to reveal the underlying distribution of artificially introduced deuterium [21]. The goal can be achieved through isotopic deconvolution of the experimental data [8,9]. Experimental data can be isotopically deconvoluted and compared with the simulated data to extract rate constants. Alternatively, simulated curves can be compared with the raw experimental data by convolution with the experimental isotopic distribution. We have adopted the second approach here.

Let the abundances of the major hydrogen/deuterium isotopomers be given by $(m), (m+1), (m+2), (m+3), \ldots, (m+i)$. If the peak shape of the multiplet given by the undeuterated isotopomer is $f(m)$, then the peak shapes of the other isotopomers will be $f(m+1), f(m+2), f(m+3), \ldots, f(m+i)$. These multiplets will be identical with the undeuterated multiplet but displaced 1, 2, 3 mass units, etc. The overall peaks as measured will be the sum of these multiplets multiplied by their abundances, that is:

$$\sum_{n=0}^{i} (m+n)\, f(m+n) \tag{1}$$

The function $f(m)$ may be established experimentally from runs at zero flow rate and the proportions of the deuterated isotopomers contributing to the products of the reaction may be deduced by combining these distributions in different proportions to give minimum sum of squares deviation from the experimental results.

This is done with the aid of the Microsoft Excel "Solver" program. It uses the generalized reduced gradient (GRG2) non-linear optimization code [22] and, in this case, optimizes $(m), (m+1), (m+2), (m+3), \ldots, (m+i)$ to minimize the squares of differences between predicted and measured overall peak patterns.

The method has the advantage of minimizing the effects of variations of isotopic ratios in natural

products. It minimizes the effects of noise and of asymmetric peak shapes and limitations of resolution in the spectra like the ones presented in Fig. 3.

3.2. Apparent and site-specific rates

Once the spectra have been deconvoluted one obtains a set of curves for consecutive deuterium exchanges, as a function of flow rate of the deuterating agent. Simulation of the kinetic data by solution of the associated set of coupled differential equations yields a set of apparent rate constants, however it is the set of site-specific rate constants that are of interest [23,24]. An algorithm based on a Modelmaker program of Cherwell Scientific solves a set of independent simultaneous differential equations for a suggested reaction mechanism and is the way for extracting site-specific rate constants that we have adopted.

For sequential reactions involving the replacement of hydrogen by deuterium one can write [8,24]

$$D_0 \xrightarrow{k_a} D_1 \xrightarrow{k_b} D_2 \quad (2)$$

where D_0, D_1 and D_2 denote molecules containing 0, 1 and 2 deuterium atoms in place of hydrogen atoms, respectively, irrespective of the deuteration site, and the rate constants are k_a and k_b. For parallel reactions of two site-specific reactions, there will be two alternative sequences:

$$A(H_aH_b) \xrightarrow{k_1} A(H_aD_b) \xrightarrow{k_2} A(D_aD_b) \quad (3a)$$

and

$$A(H_aH_b) \xrightarrow{k_2} A(D_aH_b) \xrightarrow{k_1} A(D_aD_b) \quad (3b)$$

The combination of the two reaction sequences will give different kinetics. For example, the apparent first step in the sequential mechanism with an apparent rate constant k_a will be made up of the sum of the two site-specific constants k_1 and k_2.

Modelmaker 3 solves the simultaneous first-order differential equations corresponding to an assumed mechanism by the Runge–Kutta method. If one sets up a sequence of reactions both parallel and sequential, the program will predict the concentrations of the various intermediates and products if given the appropriate rate constants. Conversely, given experimental data, it will determine the optimum rate constants by one of the standard non-linear regression methods [8]. The measure of fit between experiment and theory is the value of the correlation coefficient R^2 that should be in excess of 0.8.

Overall rate coefficients can also be obtained by monitoring the intensity of the primary ion decay as a function of the neutral gas B concentration introduced downstream.

4. Results and discussion

Protonated L-serine, $(\text{L-serine}+\text{H})^{1+}$ was produced by electrospray ionization and was injected into the flow tube. We reacted this ion in the flow tube with either ND_3 or CH_3OD and monitored the incorporation of deuterium as a function of flow rate of the deuterating reagent at a constant reaction time. All of the experiments were carried out under thermal, room temperature conditions. Five H/D exchange reactions were observed at relatively low ND_3 flow rates (up to $\sim 4.2 \times 10^{17}$ molecules s^{-1}). The results are presented in Fig. 4. Protonated L-serine is also reactive with CH_3OD and undergoes H/D exchange. The results are presented in Fig. 5. As noted earlier four exchanges were easily observed and a fifth one was only observed when much higher flow rates were employed for CH_3OD than for ND_3 (up to $\sim 1.8 \times 10^{18}$ molecules s^{-1}).

The experimental points presented in Figs. 4 and 5 are the raw data points for H/D exchange. The curves are the result of simulation of the kinetic data by solution of the associated set of differential equations (see under Section 3.2). The simulations presented involve site-specific rate constants. Overall disappearance rate constants were deduced from semilogarithmic decay plots of the reactant ion (see, for example, Fig. 6). Table 1 summarizes the rate constants obtained.

The rate constants for ND_3 are about an order of magnitude higher than for CH_3OD. This is expected in view of the much higher proton affinity of ammonia

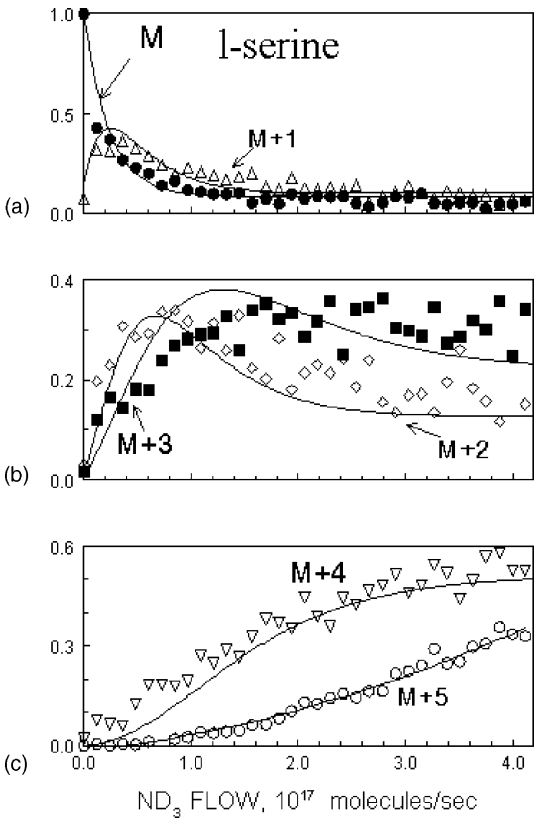

Fig. 4. Relative abundance vs. neutral flow rate for the various indicated cations in the reaction of protonated L-serine with ND_3. The relative abundances given by the symbols are the raw experimental data for $M = 106$, $M + 1 = 107$, etc. The curves are the simulated fits for derivation of site-specific H/D exchange rate constants convoluted with the natural isotopic abundance contributions of ^{13}C, ^{18}O, and ^{15}N from the dashed lines of Fig. 3. The correlation factor R^2 is 0.91.

(204 kcal mol^{-1}) compared to that of methanol (181.9 kcal mol^{-1}) [25]. ND_3 is basic enough to gain a proton and be solvated by serine whereas CH_3OD is incapable of deprotonating serine and is postulated to exchange via a "relay mechanism," in which protonated serine simultaneously gains a D while losing an H [23c]. The sum of the site-specific rate constants for the reactions of ND_3 (Table 1), $\sum k_{\text{site-specific}} = 5.9 \times 10^{-10}$ cm^3 per molecule s^{-1} is in excellent agreement with the overall rate constant, $k_{\text{semilog plot}} = 6.1 \times 10^{-10}$ cm^3 per molecule s^{-1}. The agreement is not as good in the case of CH_3OD.

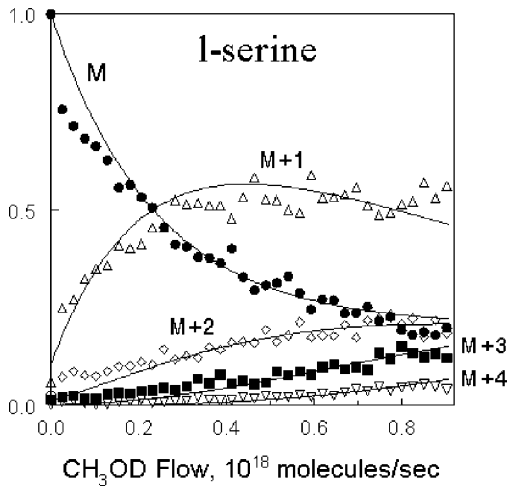

Fig. 5. Relative abundance vs. neutral flow rate for the various indicated cations in the reaction of protonated L-serine with CH_3OD (see caption to Fig. 4). The correlation factor R^2 is 0.95.

However, the site-specific rate constants for the reactions of CH_3OD indicate quite clearly three equal rates, namely three equivalent sites. This agrees with the results of DFT calculations [19], namely that the

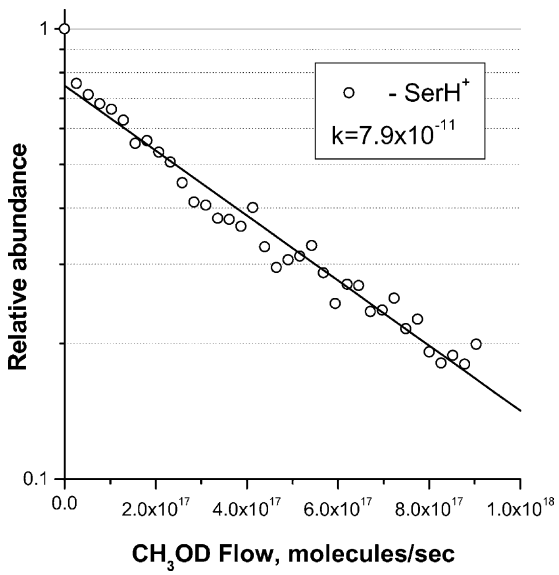

Fig. 6. Semilogarithmic plot of the decay of primary ions as a function of the neutral flow rate for the reaction of protonated L-serine with CH_3OD.

Table 1
Apparent and site-specific H/D exchange rate constants (cm^3 per molecule s^{-1})

$k_{apparent}$	$k_{site\text{-}specific}$	$\sum k_{site\text{-}specific}$	$k_{semilog\ plot}$
Serine with ND_3			
3.2×10^{-10}	4.0×10^{-10}	5.9×10^{-10}	6.1×10^{-10}
1.1×10^{-10}	6.7×10^{-11}		
7.5×10^{-11}	7.3×10^{-11}		
6.0×10^{-11}	4.7×10^{-11}		
1.0×10^{-12}			
Serine with CH_3OD			
2.6×10^{-11}	4.1×10^{-11}	4.7×10^{-11}	7.9×10^{-11}
5.2×10^{-12}	1.9×10^{-12}		
1.3×10^{-11}	1.9×10^{-12}		
7.4×10^{-12}	1.9×10^{-12}		

most stable structures of protonated serine arise from protonation of the amino group leading to an NH_3^+ group with three equivalent protons. The complexation that becomes possible in the case of ND_3 makes the assignment of site-specific rate constants less clear because more than one site can undergo exchange during the lifetime of a single collision complex. Multiple exchanges in a single collision event have been reported to be prevalent with ND_3 [26].

The single high site-specific rate constant observed for both ND_3 as well as CH_3OD can be due to either the carboxyl or the side-chain hydroxyl groups (Scheme 1). Unfortunately, we have until now been unable to extract with confidence five site-specific rate constants. The ND_3 reaction data could be fit with the following five site-specific rate constants (cm^3 per molecule s^{-1}): 3.3×10^{-11}, 3.5×10^{-11}, 4.7×10^{-11}, 9.1×10^{-11}, 3.7×10^{-10}, however with a low correlation coefficient $R^2 = 0.76$. On the other hand the fit with four site-specific rate constants 4.7×10^{-11}, 6.7×10^{-11}, 7.3×10^{-11}, 4.0×10^{-10}, (Fig. 4 and Table 1) has a correlation factor $R^2 = 0.91$.

It is instructive to compare the present results with previous results for the reaction of protonated glycine with CH_3OD [23c]. The single fast rate constant for [glycine + H^+]$^+$/CH_3OD has been determined to be 6.6×10^{-11} cm^3 per molecule s^{-1}, just slightly higher than the value determined for serine, 4.1×10^{-11} cm^3 per molecule s^{-1}. The three equal

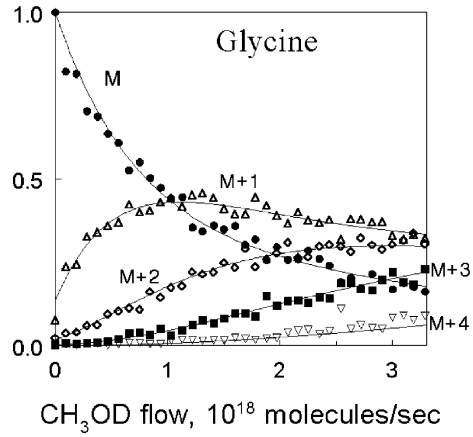

Fig. 7. Relative abundance vs. neutral flow rate for the various indicated cations in the reaction of protonated glycine with CH_3OD. The relative abundances given by the symbols are the raw experimental data for $M = 76$, $M + 1 = 77$, etc. The correlation factor R^2 is 0.96.

site-specific rate constants in glycine were found to be 8×10^{-12} cm^3 per molecule s^{-1}. Since these values are somewhat different from the ones we found for serine, we ran an experiment on glycine. The results are presented in Fig. 7. They can be modeled with three equal site-specific rate constants, 1.5×10^{-12} cm^3 per molecule s^{-1} each, and one higher rate constant, 3.6×10^{-11} cm^3 per molecule s^{-1}, in quite good agreement with the serine data. It would thus seem that we are sampling the carboxyl group in the serine reaction system and that our site-specific rate constants are somewhat lower than the ones determined by Green and Lebrilla [23c] using low-pressure FT-ICR. This is plausible if the ions are internally cooler in the flow tube experiment.

Acknowledgements

This work was supported by the United States–Israel Binational Science Foundation under grant no. 2000026. Professor Alan G. Marshall is the American cooperative investigator. The Farkas Research Center is supported by the Minerva Gesellschaft für die Forschung GmbH München.

References

[1] W. Federer, H. Ramler, H. Villinger, W. Lindinger, Phys. Rev. Lett. 54 (1985) 540.
[2] A. Hansel, R. Richter, W. Lindinger, E.E. Ferguson, Int. J. Mass Spectrom. Ion Process. 94 (1989) 251.
[3] W. Lindinger, A. Hansel, A. Jordan, Int. J. Mass Spectrom. Ion Process. 173 (1998) 191.
[4] C.S. Hoaglund-Hyzer, A.E. Counterman, D.E. Clemmer, Chem. Rev. 99 (1999) 3037.
[5] G. Koster, M. Soskin, M. Peres, C. Lifshitz, Int. J. Mass Spectrom. 179/180 (1998) 165.
[6] G. Koster, C. Lifshitz, Int. J. Mass Spectrom. 182/183 (1999) 213.
[7] G. Koster, C. Lifshitz, Int. J. Mass Spectrom. 195/196 (2000) 11.
[8] E. Levi-Seri, G. Koster, A. Kogan, K. Gutman, B.G. Reuben, C. Lifshitz, J. Phys. Chem. A 105 (2001) 5552.
[9] P. Ustyuzhanin, A. Kogan, B.G. Reuben, C. Lifshitz, Int. J. Chem. Kin. 33 (2001) 707.
[10] A. Kogan, P. Ustyuzhanin, B.G. Reuben, C. Lifshitz, Int. J. Mass Spectrom. 213 (2002) 1.
[11] J.B. Fenn, M. Mann, C.K. Meng, S.F. Wong, C.M. Whitehouse, Mass Spectrom. Rev. 9 (1990) 37.
[12] C.K. Meng, J.B. Fenn, Org. Mass Spectrom. 26 (1991) 542.
[13] M. Busman, D.R. Knapp, K.L. Schey, Rapid Commun. Mass Spectrom. 8 (1994) 211.
[14] D. Zhang, L. Wu, K.J. Koch, R.G. Cooks, Eur. Mass Spectrom. 5 (1999) 353.
[15] R.G. Cooks, D. Zhang, K.J. Koch, F.G. Gozzo, M.N. Eberlin, Anal. Chem. 73 (2001) 3646.
[16] A.E. Counterman, A.E. Hilderbrand, C.A. Srebalus Barnes, D.E. Clemmer, J. Am. Soc. Mass Spectrom. 12 (2001) 1020.
[17] J.A. Loo, Mass Spectrom. Rev. 16 (1997) 1.
[18] E.P. Hunter, S.G. Lias, J. Phys. Chem. Ref. Data 27 (3) (1998) 413.
[19] M. Noguera, L. Rodríguez-Santiago, M. Sodupe, J. Bertran, J. Mol. Struct. (Theochem.) 537 (2001) 307.
[20] N.N. Dookeran, A.G. Harrison, J. Mass Spectrom. 30 (1995) 666.
[21] Z. Zhang, S. Guan, A.G. Marshall, J. Am. Soc. Mass Spectrom. 8 (1997) 659.
[22] L. Lasdon, A. Waren, Microsoft Knowledge Base XL: Solver Uses Generalized Reduced Gradient Algorithm (Q82890).
[23] (a) E. Gard, D. Willard, J. Bregar, M.K. Green, C.B. Lebrilla, Org. Mass Spectrom. 28 (1993) 1632;
(b) M.K. Green, S.G. Penn, C.B. Lebrilla, J. Am. Soc. Mass Spectrom. 6 (1995) 1247;
(c) M.K. Green, C.B. Lebrilla, Mass Spectrom. Rev. 16 (1997) 53.
[24] F. He, A.G. Marshall, J. Phys. Chem. A 104 (2000) 562.
[25] S.G. Lias, J.E. Bartmess, J.F. Liebman, J.L. Holmes, R.D. Levin, W.G. Mallard, J. Phys. Chem. Ref. Data 17 (1) (1988) 1.
[26] S. Campbell, M.T. Rodgers, E.M. Marzluff, J.L. Beauchamp, J. Am. Chem. Soc. 116 (1994) 9765.